

1 **Yellow fever disease severity and endothelial dysfunction are associated with elevated serum**  
2 **levels of viral NS1 protein and syndecan-1**

3  
4 Francielle T. G. de Sousa<sup>1,2</sup>, Colin M. Warnes<sup>1</sup>, Erika R. Manuli<sup>2,3</sup>, Arash Ng<sup>4</sup>, Luiz G. F. A. B.  
5 D'Elia Zanella<sup>5,6</sup>, Yeh-Li Ho<sup>5</sup>, Samhita Bhat<sup>1</sup>, Camila M. Romano<sup>2,3</sup>, P. Robert Beatty<sup>1,4</sup>, Scott B.  
6 Biering<sup>1</sup>, Esper G. Kallas<sup>5</sup>, Ester C. Sabino<sup>2,5</sup>, Eva Harris<sup>1,4</sup>

7  
8 <sup>1</sup>Division of Infectious Diseases and Vaccinology, School of Public Health, University of  
9 California, Berkeley, Berkeley, CA, USA

10 <sup>2</sup>Departamento de Doenças Infecciosas e Parasitárias, Instituto de Medicina Tropical, Faculdade  
11 de Medicina da Universidade de São Paulo, São Paulo, SP, 05403000, Brazil

12 <sup>3</sup>Laboratório de Investigação Médica, Hospital das Clínicas da Faculdade de Medicina da  
13 Universidade de São Paulo (HCFMUSP), São Paulo-SP, 05403000, Brazil

14 <sup>4</sup>Department of Molecular and Cell Biology, University of California, Berkeley, Berkeley, CA,  
15 USA

16 <sup>5</sup>Hospital das Clínicas da Faculdade de Medicina da Universidade de São Paulo (HCFMUSP),  
17 São Paulo-SP, 05403000, Brazil

18 <sup>6</sup>Instituto de Infectologia Emílio Ribas, São Paulo-SP, 01246-900, Brazil

19  
20 Correspondence to Ester C. Sabino ([sabinoec@usp.br](mailto:sabinoec@usp.br)) and Eva Harris ([eharris@berkeley.edu](mailto:eharris@berkeley.edu))

21

22 **Abstract**

23 Yellow fever virus (YFV) infections can cause severe disease manifestations, including hepatic  
24 injury, endothelial damage, coagulopathy, hemorrhage, systemic organ failure, and shock, and are  
25 associated with high mortality in humans. While nonstructural protein 1 (NS1) of the related  
26 dengue virus is implicated in contributing to vascular leak, little is known about the role of YFV  
27 NS1 in severe YF and mechanisms of vascular dysfunction in YFV infections. Here, using serum  
28 samples from qRT-PCR-confirmed YF patients with severe (n=39) or non-severe (n=18) disease  
29 in a well-defined hospital cohort in Brazil, plus samples from healthy uninfected controls (n=11),  
30 we investigated factors associated with disease severity. We developed a quantitative YFV NS1  
31 capture ELISA and found significantly increased levels of NS1, as well as syndecan-1, a marker  
32 of vascular leak, in serum from severe YF as compared to non-severe YF or control groups. We  
33 also showed that hyperpermeability of endothelial cell monolayers treated with serum from severe  
34 YF patients was significantly higher compared to non-severe YF and control groups as measured  
35 by transendothelial electrical resistance (TEER). Further, we demonstrated that YFV NS1 induces  
36 shedding of syndecan-1 from the surface of human endothelial cells. Notably, YFV NS1 serum  
37 levels significantly correlated with syndecan-1 serum levels and TEER values. Syndecan-1 levels  
38 also significantly correlated with clinical laboratory parameters of disease severity, viral load,  
39 hospitalization, and death. In summary, this study points to a role for secreted NS1 in YF disease  
40 severity and provides evidence for endothelial dysfunction as a mechanism of YF pathogenesis in  
41 humans.

42

43 **Keywords:** yellow fever, pathogenesis, endothelial dysfunction, NS1, syndecan-1

44

45 **Significance**

46 Yellow fever virus (YFV) infections cause a major global disease burden, and as such it is critical  
47 to identify clinical correlates of disease severity. Using clinical samples from our hospital cohort  
48 in Brazil, we show that YF disease severity is associated with increased serum levels of the viral  
49 nonstructural protein 1 (NS1) and soluble syndecan-1, a marker of vascular leak. This study  
50 extends the role of YFV NS1 in triggering endothelial dysfunction to human YF patients,  
51 previously demonstrated *in vitro* and in mouse models. Further, we developed a YFV NS1-capture  
52 ELISA that serves as a proof-of-concept for low-cost NS1-based diagnosis/prognosis tools for YF.  
53 Together, our data shows that YFV NS1 and endothelial dysfunction are important components of  
54 YF pathogenesis.

55

## 56 Introduction

57 Yellow fever virus (YFV) is an arbovirus endemic to tropical areas of Central and South America  
58 and sub-Saharan Africa and the causative agent of yellow fever (YF) disease. YF is considered a  
59 reemerging disease, with increasing infections over the past 20 years, exemplified by epidemics in  
60 2015 and 2016 in Angola and the Democratic Republic of Congo and in 2016-2019 in Brazil (1,  
61 2). The clinical spectrum of YF in humans ranges from asymptomatic infection to mild illness to  
62 severe disease. Manifestations of severe disease include vasculopathy and organ impairment of the  
63 liver, kidneys, lungs, intestine, and brain, resulting in high reported case fatality rates (20-60%)  
64 (2).

65  
66 YFV is a member of the *Flavivirus* genus of the *Flaviviridae* family, with a positive-sense RNA  
67 genome of approximately 11 kb that encodes three structural and seven nonstructural proteins (3).  
68 The *Flavivirus* nonstructural protein 1 (NS1) is secreted by infected cells and has been used as a  
69 serological diagnostic marker for dengue (4). Further, dengue virus (DENV) NS1 levels have been  
70 correlated with disease severity (5–7). We have recently shown that *Flavivirus* NS1 can directly  
71 cause vascular leak *in vitro* and in animal models in a tissue-specific manner that reflects the viral  
72 disease tropism (8, 9). Mechanisms of NS1-induced endothelial dysfunction include disruption of  
73 key barriers of endothelial integrity such as the glycocalyx (8) and intercellular junctional  
74 complexes (9, 10). Further, studies have demonstrated that soluble NS1, independently from the  
75 virus, can act on endothelial cells to facilitate viral dissemination and pathology (11, 12). In  
76 addition, DENV NS1 has been shown to increase circulating levels of glycocalyx components  
77 including sialic and hyaluronic acid, heparan sulfate, and syndecan-1 (SDC-1) *in vitro*, in animal  
78 models, and in clinical samples (8, 13–18). However, while YFV NS1 can trigger endothelial  
79 dysfunction *in vitro* and in animal models (8), a direct correlation of NS1 levels with severe YF  
80 disease in humans has not been demonstrated.

81  
82 SDC-1, also known as CD138, is an extracellular matrix receptor and a member of the  
83 transmembrane heparan sulfate proteoglycan family. SDC-1 is involved in many cellular functions,  
84 including cell-cell and cell-matrix adhesion, and is highly expressed by epithelial, endothelial, and  
85 hematopoietic cells (19, 20). As a part of normal cell surface proteoglycan turnover, the  
86 ectodomain of SDC-1 is constitutively shed from the cell surface via proteolytic cleavage by

87 metalloproteinases (21). Increased levels of soluble syndecan-1 (sSDC-1) have been detected in  
88 response to injury or infection, and sSDC-1 is often utilized as a marker for glycocalyx disruption.  
89 Therefore, sSDC-1 has been identified as a potential prognostic factor in cancer and systemic  
90 inflammatory and autoimmune diseases (19, 20, 22). In addition, sSDC-1 has been associated with  
91 severe manifestations of SARS-CoV-2 infection (23, 24), and elevated levels of sSDC-1 were  
92 found in patients with severe dengue due to the destruction of the glycocalyx associated with  
93 vascular leak (16, 25). Nonetheless, to date, a link between YF disease severity and glycocalyx  
94 disruption or increased serum levels of sSDC-1 has not yet been demonstrated.

95  
96 In this study, we use a well-defined cohort of patients with YFV infection to examine the  
97 relationship between levels of YFV NS1, sSDC-1, and severe disease manifestations. We found  
98 significantly higher levels of YFV NS1 and sSDC-1 in sera of severe YF patients as compared to  
99 non-severe YF and control groups. YFV NS1 and sSDC-1 serum levels correlated with each other  
100 and with clinical laboratory signs of severe YF disease. We also found that treatment of endothelial  
101 monolayers with serum from individuals with severe YF induced significantly higher levels of  
102 endothelial permeability as compared to the non-severe YF and control groups. Further, YFV NS1  
103 treatment of endothelial cells induced syndecan shedding, as observed by immunofluorescence  
104 assay. Together, these results provide evidence for a role of NS1 in YF disease and for endothelial  
105 glycocalyx disruption as a pathogenic mechanism in YFV infections in humans.

106

## 107 **Results**

### 108 **Characteristics of study participants**

109 In this study, we analyzed serum samples from individuals with suspected YF collected at the time  
110 of hospital admission during an observational cohort study initiated during the 2018 YF epidemic  
111 in São Paulo, Brazil, as previously described (2), and continued through the subsequent epidemic  
112 in 2019. Demographic characteristics, clinical manifestations, and laboratory data of study  
113 participants with RT-PCR-confirmed YF cases as well as healthy controls are provided in Table 1.  
114 We used the laboratory criteria (viral load, neutrophil count, aspartate transaminase [AST],  
115 creatinine, and indirect bilirubin [IB]) previously determined to predict mortality in YF patients  
116 from the same cohort (2), or death, to define severe cases. Table 1 shows that in addition to these  
117 criteria, severe YF cases also displayed significantly higher levels of alanine aminotransferase

118 (ALT), total bilirubin (TB), and direct bilirubin (DB), as well as increased prothrombin time  
119 (PT/INR) and activated partial thromboplastin time (aPTT), when compared to the non-severe  
120 group. The majority of YFV-positive study participants were male agriculture or forestry workers.

121

## 122 **Development of a quantitative YFV NS1 capture ELISA for clinical samples**

123 While YFV NS1 has been previously implicated as a direct trigger of endothelial dysfunction and  
124 vascular leak *in vitro* and in mouse models (8), the contribution of YFV NS1 to endothelial  
125 dysfunction in humans is unknown. To measure YFV NS1 levels in the serum of infected patients,  
126 we established a quantitative YFV NS1 capture ELISA using an in-house-produced mouse anti-  
127 YFV-NS1 monoclonal antibody (mAb). After testing different mAbs, YFJ19 (IgG1) used as the  
128 capture mAb and biotinylated YFJ19 as the detection mAb was determined to be the optimal  
129 combination, displaying the highest signal and specificity for YFV NS1 (Supplementary Fig. 1).  
130 Standard curves were generated via ELISA with recombinant YFV NS1 concentrations (0.24–2000  
131 ng/mL) versus absorbance values (Fig. 1A), with no significant changes observed when human  
132 serum (1:10) was added (Fig. 1B), indicating that the assay could be performed with clinical  
133 samples. The analytic detection range was 2 to 500 ng/mL. YFJ19, as well as 2B7, a pan-flavivirus  
134 anti-NS1 mAb, was tested across a panel of 12 flavivirus NS1 proteins using both direct ELISA  
135 and Western blot methods. Results show that YFJ19, in contrast to 2B7, was specific to YFV NS1  
136 (Fig. 1C, D, E). This specificity is important for assays detecting flavivirus NS1, especially  
137 because different flaviviruses can co-circulate in endemic areas such as Brazil.

138

## 139 **NS1 serum levels are significantly increased in severe YF**

140 Using our in-house ELISA, we found that YFV NS1 levels were significantly higher in the severe  
141 YF group (mean=118.8 ng/mL) compared to the non-severe group (mean=29.5 ng/mL) and to the  
142 control group (no NS1 detected) (Fig. 2A). We also observed trending higher levels of YFV NS1  
143 when comparing the deceased to the surviving group (Fig. 2B). YFV NS1 serum levels were  
144 observed to be highest between 5-13 days post-symptoms onset (Fig. 2C).

145

## 146 **Serum levels of syndecan-1 correlate with disease severity in YF patients**

147 Because sSDC-1 is a biomarker for endothelial injury in multiple diseases, we quantified sSDC-1

148 in the serum samples of our cohort. We found significantly increased sSDC-1 levels in severe vs.  
149 non-severe YF cases and significantly higher levels in both non-severe and severe YF groups when  
150 compared to healthy controls (Fig. 3A). Importantly, sSDC-1 levels were also significantly higher  
151 in individuals who succumbed compared to those who survived (Fig. 3B). These findings indicate  
152 that endothelial dysfunction is associated with disease severity in YFV-infected patients and that  
153 sSDC-1 can be used as a biomarker of YF disease severity. Similar to YFV NS1, sSDC-1 serum  
154 levels were highest 4-13 days after symptom onset (Fig. 3C). We also found that, as expected,  
155 sSDC-1 levels when compared to the same healthy controls as above were significantly increased  
156 in serum samples from dengue patients with diagnosed vascular leak obtained in our previous  
157 study (26) (Fig. 3D).

158

### 159 **Sera from patients acutely infected with YFV induce endothelial dysfunction *in vitro*,** 160 **correlating with disease severity**

161 To evaluate the capacity of serum from YF patients to mediate endothelial hyperpermeability, we  
162 evaluated the transendothelial electrical resistance (TEER) of human endothelial cells cultured in  
163 Transwell inserts and treated with sera from the different groups. We found that mean relative  
164 TEER values of severe and non-severe YF groups were reduced in comparison to medium-only or  
165 control groups, indicating that serum components were capable of inducing varying degrees of  
166 endothelial hyperpermeability according to disease severity (Fig. 4A). Comparing the area under  
167 the curve (AUC) of TEER nadirs, the severe YF group displayed significantly greater values when  
168 compared to both non-severe YF and control groups (Fig. 4B). Similarly, recombinant YFV NS1,  
169 used as positive control, induced endothelial dysfunction resulting in reduction of relative TEER  
170 values (Fig. 4A, B). The TEER curves for each sample are shown in Supplementary Fig. 2.

171

### 172 **YFV NS1 induces sSDC-1 shedding in endothelial cells**

173 To evaluate the capacity of YFV NS1 to serve as a direct trigger of endothelial dysfunction, we  
174 measured the effect of NS1 on SDC-1 levels on a monolayer of human endothelial cells. Consistent  
175 with our observed correlation between YFV NS1 and sSDC-1 in clinical samples, we found that  
176 YFV NS1 treatment of endothelial cells resulted in a significant reduction of cell surface-bound  
177 SDC-1 relative to medium only control (Fig. 4C, D, E). These data support a direct role for YFV

178 NS1 as a contributing factor to endothelial dysfunction in YF patients.

179

### 180 **TEER, sSDC-1, and YFV NS1 serum levels correlate with parameters of severe YF**

181 We next performed a correlation matrix analysis of patient data and results regarding TEER, sSDC-  
182 1 and YFV NS1 levels (Fig. 5A, with significant [ $p < 0.05$ ,  $r > 0.35$ ] correlations indicated with  
183 asterisks). Importantly, we found that YFV NS1 levels correlated with sSDC-1 levels, TEER  
184 values, neutrophil count, hematocrit (Ht), and IB (Fig. 5A, B, C). Further, sSDC-1 levels correlated  
185 significantly with YFV NS1, TEER values, gender, hospitalization, viral load, parameters of liver  
186 impairment (AST, ALT, creatinine, TB, DB, and IB), kidney dysfunction (creatinine),  
187 coagulopathy (fibrinogen, PT/INR, aPTT), and death (Fig. 5A, D). TEER values correlated with  
188 YFV NS1, sSDC-1, gender, creatinine, TB, DB, and IB (Fig. 5A, C, D). Thus, these findings show  
189 that TEER values and levels of YFV NS1 and sSDC-1 correlated with each other and with clinical  
190 laboratory parameters of disease severity, suggesting a potential link between YFV NS1 and  
191 endothelial dysfunction, resulting in increased shedding of sSDC1.

192

### 193 **Discussion**

194 Our findings in this study indicate that in humans, YFV NS1 may directly target the endothelium,  
195 triggering breakdown of the glycocalyx via enzymatic activation, consistent with our previous  
196 report using *in vitro* and *in vivo* models (8). Serum levels of both NS1 and sSDC-1 were correlated  
197 with several clinical laboratory parameters associated with YF disease, providing evidence that  
198 YFV NS1 and sSDC-1 may be linked to severe YF disease manifestations. When placing human  
199 endothelial cells in contact with sera from the different groups, we observed a significant increase  
200 in permeability with the severe as compared to non-severe and healthy control groups. We also  
201 confirmed *in vitro* by IFA that YFV NS1 induces shedding of sSDC-1 from human endothelial  
202 cells. Our results highlight the secretion of YFV NS1 from infected cells and endothelial  
203 glycocalyx degradation, as measured by sSDC-1 shedding, as prominent characteristics of YF  
204 pathogenesis in humans and suggest that levels of NS1 and/or levels of sSDC-1 may help assess  
205 risk of developing severe illness.

206

207 Flavivirus NS1 is an important virulence factor in facilitating flavivirus pathogenesis by triggering



208 enzymatic disruption of the glycocalyx as well as mediating the breakdown of intercellular  
209 junctional complexes of endothelial cells, both pathways contributing to tissue-specific vascular  
210 leak (8, 9, 27). We have previously shown that YFV NS1 treatment induces significant  
211 hyperpermeability in human endothelial cells and in mice (8). Our data here shows that severe YF  
212 cases displayed higher levels of YFV NS1 as early as 5 days post-disease onset, supporting the  
213 concept that production of NS1 by YFV-infected cells may contribute to YF disease. Thus,  
214 measuring the serum levels NS1 could potentially provide a clinical diagnostic/prognostic marker  
215 for YF.

216  
217 SDC-1 is a heparan sulfate proteoglycan expressed on endothelial cells and an established marker  
218 of inflammatory disease and glycocalyx damage (28). Shedding of endothelial glycocalyx  
219 components, such as sSDC-1, is a known result of endothelial dysfunction, and increased serum  
220 levels of sSDC-1 have been confirmed in patients with diseases such as dengue (16, 25, 29, 30),  
221 COVID-19 (24), septic shock (31), and cancer (32, 33). Here, we show that higher levels of sSDC-  
222 1 correlate with severe YF; thus, sSDC-1 may also serve as a biomarker for severe YF disease.

223  
224 YF is a systemic disease, but the pathology is primarily targeted to the liver. A recent study  
225 highlighted endothelial activation, showing immunohistochemical analysis of endothelial tissues  
226 in the hepatic parenchyma of YF-positive subjects, with increased expression of adhesion  
227 molecules (34). This study suggested that YFV induces endothelial activation, stimulating the  
228 rolling, recruitment, and migration of immune cells that contribute to inflammatory processes in  
229 the liver of fatal cases. Our current results highlight secretion of YFV NS1 into the bloodstream,  
230 where it presumably interacts with the endothelium, activating glycocalyx degradation and SDC-  
231 1 shedding that leads to endothelial hyperpermeability and possibly contributing to the hepatic and  
232 systemic inflammatory response.

233  
234 In a previous study by Kallas et al. (2019), older age, male sex, higher leukocyte and neutrophil  
235 counts ( $>4000$  cells/ mL), AST, bilirubin, creatinine, and viral load ( $>5.1$  log<sub>10</sub> copies/mL), as  
236 well as prolonged prothrombin time, were associated with increased mortality in patients with YF  
237 (2). Thus, we used these parameters to classify severe cases of YF in our current study, which  
238 utilized samples obtained from the same cohort. In a more recent study, hyperimmune activation

239 and perturbation of the gut microbiome related to heightened levels of microbial translocation were  
240 also found to be associated with severe outcome in these patients (35). Moreover, coagulopathy in  
241 YF patients from the same cohort and in YFV-infected macaques was not only associated with  
242 defects in clotting factor synthesis due to hepatocyte infection, but also with coagulation factor  
243 consumption, shown by increased concentrations of plasma D-dimer (36).

244  
245 Antigenic cross-reactivity during diagnosis of flaviviral diseases is a major challenge, particularly  
246 in endemic settings where multiple flaviviruses co-circulate (37). Therefore, assays measuring  
247 NS1 in sera must be highly specific to avoid incorrect diagnosis. The presence of NS1 is widely  
248 used as an early diagnostic marker for flavivirus infections, especially dengue (38). We produced  
249 and tested multiple novel anti-YFV NS1 mAbs when developing our YFV NS1 capture ELISA,  
250 aiming for minimal cross-reactivity to other flavivirus NS1 proteins while maintaining the highest  
251 sensitivity possible. Because our newly developed YFV NS1 ELISA is highly specific and can  
252 detect low concentrations of NS1 in supernatants or sera, it could be used in research and clinical  
253 settings, including differential diagnosis of flaviviruses at lower cost compared to molecular  
254 assays, with additional potential for prognosis.

255  
256 Taken together, our study identifies YFV NS1 and sSDC-1 as correlates of YF disease severity and  
257 endothelial dysfunction. Our work suggests that endothelial dysfunction is a major clinical  
258 manifestation of human YF, as in dengue, and that circulating NS1 may contribute to this  
259 pathogenesis, as has been observed *in vitro* and in murine models. Further, our development of a  
260 highly specific YFV NS1 capture ELISA can serve as a proof-of-concept for the development of  
261 low-cost NS1-based diagnostics of YF and perhaps be used to predict YF disease progression in  
262 humans.

263

## 264 **Methods**

### 265 **Study participants**

266 This study utilized samples from patients with YF cases confirmed by detection of YFV genomic  
267 RNA in plasma and/or autopsy tissues by qRT-PCR, as previously described (2). Patients were  
268 enrolled at the Hospital das Clínicas, School of Medicine, University of São Paulo, Brazil, during  
269 an observational cohort study from January 2018 through February 2019 (2). Blood samples were

270 collected at the time of admission after informed consent and before any treatment intervention or  
271 diagnostic procedure. Blood samples were used for clinical laboratory tests including  
272 determination of viral load; leukocyte and platelet counts; levels of hemoglobin, AST, ALT,  
273 creatinine, fibrinogen, and total, direct, and indirect bilirubin; and coagulation time. Cases were  
274 classified in three groups, as follows: i) non-severe (N=18): individuals who presented viral load  
275  $<10^5$  genomic copies/mL, neutrophil count  $<4000$ /mL, AST  $<3500$  U/L, creatinine  $<2.36$  mg/mL,  
276 and IB  $<0.64$  mg/dL and who recovered; ii) severe (N=39): individuals who presented one or more  
277 of the following criteria: viral load  $\geq 10^5$  genomic copies/mL; neutrophil count  $\geq 4000$ /mL, AST  
278  $\geq 3500$  U/L, creatinine  $\geq 2.36$  mg/mL, IB  $\geq 0.64$  mg/dL, and/or death; iii) control (N=11): healthy  
279 individuals. The study was approved by the Institutional Review Board of the University of São  
280 Paulo (approval # CAAE: 59542216.3.1001.0068).

281

## 282 **Hybridoma production and ELISA and Western blot analysis**

283 BALB/c mice were immunized intraperitoneally three times with 10  $\mu$ g of recombinant YFV NS1  
284 (Strain 17D, Native Antigen) diluted 1:1 in Sigma adjuvant system, and a fourth immunization  
285 with YFV NS1 alone. Splenocytes were fused with A1 myeloma cells, and hybridomas were  
286 selected on hypoxanthine-aminopterin-thymidine medium and screened with a YFV NS1 antigen-  
287 coat ELISA. In brief, Nunc MaxiSorp ELISA plates (Thermo Scientific) were coated overnight  
288 with 0.5  $\mu$ g/mL of YFV NS1 in PBS and blocked the next day for 1 hour (h) using PBS containing  
289 5% nonfat dry milk, washed twice with PBS, and incubated with hybridoma supernatant for 1h at  
290 room temperature. Plates were washed 3X with PBS-Tween20 0.01% (PBS-T) and 2X with PBS,  
291 and HRP-conjugated secondary antibody diluted in PBS-BSA 1% was added for 1h. After washing  
292 with PBS-T, 3,3',5,5'-Tetramethylbenzidine (TMB) liquid substrate (Sigma) was added and left to  
293 develop for 10 minutes. Plates were read at OD<sub>450</sub> nm using a BioTek/Agilent microplate reader.  
294 The mAbs with the highest OD value and shortest growth doubling time were selected for  
295 expansion and purification. Cells from ELISA-positive wells were sub-cloned and expanded  
296 before being tested by ELISA for YFV specificity using 12 recombinant flavivirus NS1 proteins  
297 purchased from Native Antigen Company: YFV; dengue virus serotypes 1 (DENV1), 2 (DENV2),  
298 3 (DENV2), and 4 (DENV4); Saint Louis encephalitis virus (SLEV); West Nile virus (WNV);  
299 Zika virus (ZIKV); Wesselsbron virus (WBV); Usutu virus (USUV); Japanese encephalitis virus  
300 (JEV); and tick-borne encephalitis virus (TBEV) (31).

301  
302 The YFJ19 mAb was tested by Western blot for specificity to YFV NS1. The same 12 recombinant  
303 flavivirus NS1 proteins used above were separated on a 10% polyacrylamide gel and transferred  
304 onto nitrocellulose membranes. Membranes were incubated overnight with 7 mL of hybridoma  
305 supernatant or 3.5  $\mu$ L of mouse anti-His mAb (Abcam) as a control in PBS-T containing 5% nonfat  
306 dry milk. After antibody incubation, membranes were washed 4X with PBS-T and then probed  
307 with anti-mouse secondary antibodies conjugated to horseradish peroxidase (HRP; Biolegend) for  
308 1h. Membranes were then washed 4X with PBS-T, developed using ECL reagents, imaged on a  
309 ChemiDoc system, and analyzed using Image Lab software (Bio-Rad).

### 310 311 **mAb purification**

312 Hybridoma supernatant in batches of 400 mL were filtered using a 0.22  $\mu$ m pore size bottle-top  
313 vacuum filter (Corning) to remove cell debris. Buffers were developed based on the manufacturer's  
314 recommendations (Cytiva Protein G Sepharose 4 Affinity Chromatography Handbook).  
315 Supernatant was diluted 1:1 with binding buffer (20 mM  $\text{H}_2\text{NaO}_4\text{P}\cdot\text{H}_2\text{O}$ , pH 7.0). Protein G resin  
316 (2.5 mL, Cytiva Protein G Sepharose<sup>TM</sup> 4 Fast Flow) was added to a 1.0 x 10 cm Econo-Column  
317 (Bio-Rad) and washed twice with 10 mL of binding buffer. Supernatant/binding buffer solution  
318 was added to a Econo-Column Reservoir (Bio-Rad) attached to the Econo-Column and allowed to  
319 gravity flow through the resin. After flow-through was collected, the resin was washed twice with  
320 10 mL of binding buffer to remove supernatant. To elute the bound mAbs, 6 mL of elution buffer  
321 (0.1 M glycine buffer, pH 2.5-3.0) was added to the column. Elution fractions were collected in 1-  
322 mL fractions and diluted 1:10 with neutralizing buffer (1 M TrisHCl, pH 9.0). mAb concentration  
323 was calculated using a Nanodrop spectrophotometer, and the top yields were selected and pooled.  
324 Purified mAbs were dialyzed using a Slide-A-Lyzer 10K (Fisher) over 48h at 4°C with two  
325 separate exchanges of PBS buffer.

### 326 327 **YFV NS1 capture ELISA**

328 ELISA plates were coated with 5  $\mu$ g/mL of capture mAb in 50  $\mu$ L PBS/well and incubated at 4°C  
329 overnight. The next day, plates were washed once with PBS and blocked with PBS-BSA 3% (100  
330  $\mu$ L) and incubated for 1h at room temperature. The plate was then washed twice with PBS-T, and  
331 the serum or recombinant NS1 was diluted in PBS-BSA 1% (50  $\mu$ L) before being added to the

332 plate and incubated for 1h at room temperature. Plates were washed 4X with PBS-T, and the  
333 biotinylated detecting mAb (Pierce Antibody Biotinylation Kit for IP, ThermoFisher) was diluted  
334 in PBS-BSA 1% (50  $\mu$ L) and added to the plate to incubate for 1h at room temperature. The plate  
335 was then washed 4X with PBS-T. HRP-streptavidin (Jackson Immuno) diluted in PBS-BSA (50  
336  $\mu$ L) was then added to the plate and incubated at room temperature for 1h. After incubation, the  
337 plate was washed 4X with PBS-T and 1X with PBS. The plate was then developed with TMB  
338 substrate (100  $\mu$ L; Sigma) for ~15 minutes. The enzymatic reaction was interrupted using 2N  
339 H<sub>2</sub>SO<sub>4</sub>, and the plate was read at OD<sub>450</sub> nm. The concentrations of NS1 in sera were interpolated  
340 using a standard curve of recombinant NS1 ranging from 1 to 1000 ng/mL; the limit of detection  
341 for this assay was 2 ng/mL.

342

#### 343 **Determination of sSDC-1 levels in human serum**

344 The amount of sSDC-1 in serum was determined using the human SDC-1 DuoSet ELISA Kit  
345 (DY2780, R&D Systems). Briefly, 96-well ELISA microplates were coated with 80 ng/well of  
346 goat anti-human SDC-1 capture antibody overnight at room temperature. After washing and  
347 blocking with 1% bovine serum albumin (BSA), plates were incubated with samples diluted 1:25  
348 or recombinant human SDC-1 standards for 2h. After washing, plates were incubated with 5  
349 ng/well of biotinylated goat anti-human SDC-1 detection antibody. After 2h, HRP-streptavidin was  
350 added for signal detection with TMB substrate. The OD<sub>450</sub> with a correction at OD<sub>550</sub> was  
351 determined using a microplate reader. sSDC-1 levels were determined by interpolation analysis of  
352 standard curves with four-parameter logistic regression.

353

#### 354 **Evaluation of endothelial barrier function *in vitro***

355 To evaluate the putative effects of serum from acutely YFV-infected patients on endothelial barrier  
356 function, we used the TEER assay as described previously (26, 27). In brief, human umbilical vein  
357 endothelial cells, kindly donated by Dr. Miriam Fonseca-Alaniz (Instituto do Coração, InCor,  
358 University of São Paulo, Brazil) were seeded ( $6 \times 10^4$  cells/well) in Transwell polycarbonate  
359 membrane inserts (0.4  $\mu$ m pore, 6.5 mm diameter; Corning Inc.) in endothelial cell growth basal  
360 medium 2 supplemented with an Endothelial Cell Growth Medium-2 (EGM-2TM) supplemental  
361 bullet kit (Lonza). After 72h of incubation at 37°C and 5% CO<sub>2</sub>, cells were treated with human  
362 sera (10% final vol/vol concentration) obtained from YFV-positive severe and non-severe patients

363 or YFV-negative blood donors (healthy controls). TEER values, expressed in Ohms ( $\Omega$ ), were  
364 collected at sequential 2-h time-points 2-10h following treatments using an Epithelial Volt Ohm  
365 Meter (EVOM) with a “chopstick” electrode (World Precision Instruments). Resistance of inserts  
366 with no cells (blank) and inserts with cells (untreated) containing medium alone, were used to  
367 calculate relative TEER as a ratio of the corrected resistance values as ( $\Omega$  experimental condition  
368 -  $\Omega$  blank)/( $\Omega$  untreated -  $\Omega$  blank). Recombinant YFV NS1 (Native Antigen Co.) at 10  $\mu\text{g}/\text{mL}$  was  
369 used as positive control.

370

### 371 **Measurement of SDC-1 levels on the surface of human endothelial cells by** 372 **immunofluorescence assay (IFA)**

373 HPMEC ( $1 \times 10^5$  cells) were seeded on gelatin-coated coverslips and allowed to grow until full  
374 confluency was attained (approximately 3 days). On the day of the experiment, cells were treated  
375 or not with 10  $\mu\text{g}/\text{mL}$  of YFV NS1 protein and incubated for 3h at 37°C. After incubation, cells  
376 were washed, fixed with 4% paraformaldehyde (PFA), and stained overnight with 2  $\mu\text{g}/\text{mL}$  of the  
377 rabbit anti-SDC-1 IgG antibody (Abcam, ab188861). After washing, secondary staining was  
378 performed by adding 2  $\mu\text{g}/\text{mL}$  of donkey anti-rabbit IgG conjugated to Alexa Fluor 647 (Abcam,  
379 ab150075) for 4h. Nuclei were stained using Hoechst (ImmunoChemistry Technologies). Mounted  
380 slides were imaged on a Zeiss LSM 710 Axio Observer fluorescence microscope (CRL Molecular  
381 Imaging Center, UC Berkeley). Images acquired using the Zen 2010 software (Zeiss, Jena,  
382 Germany) were processed and analyzed with ImageJ software (39). Mean fluorescence intensity  
383 (MFI) values for SDC-1 staining were obtained from individual RGB-grayscale-transformed  
384 images ( $n = 3$ ).

385

### 386 **Statistics**

387 ELISA values were modeled using 4-parametric logistic regression, which follows a sigmoidal  
388 distribution to represent the optical density range (40). Spearman's rank correlation was used to  
389 determine the relationship between two non-parametric continuous variables (41). Linear models  
390 were used to visualize the relationship between continuous values of relevant biomarkers (42).  
391 Locally estimated scatterplot smoothing (LOESS) models were used to visualize the trend of  
392 relevant biomarkers over days since symptom onset (43). LOESS models were implemented using  
393 a span = 1. The span was determined based on the best visualization that accounts for the low

394 sample size and large gaps between the sample days. Data were analyzed using R language version  
395 4.1.1 within the RStudio (2021.09.0, Build 351) integrated development environment. Plots were  
396 visualized using the base R graphics and ggplot2 (v3.3.5) package. Statistical tests used in this  
397 study include ANOVA analysis with multiple comparisons test as well as t-tests, as indicated in  
398 the figure legends. Resultant  $p$ -values from the above statistical tests are displayed as ns, not  
399 significant ( $p \geq 0.05$ ) or with asterisks as follows:  $*p < 0.05$ ,  $**p < 0.01$ ,  $***p < 0.001$ , or  
400  $****p < 0.0001$ . All statistics not indicated are not significant.

401

402

### 403 **Acknowledgments**

404 This study was supported by NIH grants, R01 AI24493 (E.H.) and R01 AI168003 (E.H.), and by  
405 São Paulo Research Foundation-FAPESP (Project #2013/01690-0 to ECS and Scholarships  
406 #2013/01702-9 and 2017/16627-3 to FTGS). SBB was supported in part as an Open Philanthropy  
407 Awardee of the Life Sciences Research Foundation.

408

409

## 410 **Figures Legends**

411

412 **Fig. 1. Development of quantitative YFV NS1 ELISA.** (A) Sigmoidal standard curve of YFV  
413 NS1 capture ELISA performed with YFJ19 mAb and thirteen different concentrations of  
414 recombinant YFV NS1. (B) Comparison of standard curve of YFV NS1 diluted or not in normal  
415 human serum (1:10). (C) Specificity of mAb YFJ19 by direct ELISA performed with NS1 (5  
416 ug/mL) from 12 different flaviviruses as follows: YFV; dengue virus serotypes 1 (DENV1), 2  
417 (DENV2), 3 (DENV2), and 4 (DENV4); Saint Louis encephalitis virus (SLEV); West Nile virus  
418 (WNV); Zika virus (ZIKV); Wesselsbron virus (WBV); Usutu virus (USUV); Japanese  
419 encephalitis virus (JEV); Tick-borne encephalitis virus (TBEV). (D) Cross-reactivity an anti-  
420 flavivirus NS1 mAb (2B7) by direct ELISA performed with NS1 (5 ug/mL) from the 12 different  
421 flaviviruses as in C. (E) Western blot analysis showing specificity of mAb YFJ19 for YFV NS1.

422

423 **Fig. 2. YFV NS1 serum levels in severe and non-severe YF patients.** (A) YFV NS1 levels were  
424 determined using an in-house sandwich ELISA, as described in Materials and Methods. Studied  
425 individuals were classified in three different groups as described in Materials and Methods: 1)  
426 Severe YF (n=39); non-severe YF (n=16); controls (n=5): healthy individuals. (B) YFV NS1 levels  
427 in survivors and deceased YFV-infected groups. Mean ranks of groups were compared by Mann-  
428 Whitney test (significance level of 0.05). (C) YFV NS1 serum levels in individuals with acute YF  
429 according to days since symptom onset, visualized using a LOESS model.

430

431 **Fig. 3. sSDC-1 levels in sera of individuals with acute YF and dengue.** (A) The sSDC-1 levels  
432 in sera were determined by the Human sSDC-1 ELISA Kit. Studied individuals were classified in  
433 three different groups as described in Materials and Methods: 1) Severe YF (n=39); non-severe YF  
434 (n=18); controls (n=11): healthy individuals. (B) sSDC-1 serum levels in survivors and deceased  
435 YFV-infected groups. (C) Distribution and average (solid lines) of sSDC-1 serum levels in  
436 individuals with acute YF according to days since symptoms onset, visualized using a LOESS  
437 model. (D) sSDC-1 serum levels in individuals with acute DENV infection. Dengue no leak (n=7):  
438 individuals with acute dengue who did not display plasma leakage; Dengue leak (n=7): individuals  
439 with acute dengue who displayed plasma leakage; Controls (n=11): same healthy individuals  
440 shown in panel A. Mean ranks of sSDC-1 levels of YF or dengue groups were compared by



441 Kruskal-Wallis + Dunn's multiple comparisons test. Median of sSDC-1 levels in deceased and  
442 survived patients were compared Mann Whitney test (significance level of 0.05).

443

444 **Fig. 4. Relative TEER of human endothelial cells treated with acute YF human serum**  
445 **samples and IFA of SDC-1 after NS1 treatment.** (A) Confluent monolayers of human endothelial  
446 cells cultured in Transwell inserts were treated or not with 10% serum from three different groups:  
447 1) Severe YF (n=24); Non-severe YF (n=10); Controls (n=11): healthy individuals. YFV NS1 (10  
448 ug/mL) was used as positive control. The transendothelial electrical resistance (TEER) was  
449 measured from 2 to 10h post-treatment. Graph shows mean  $\pm$  SD of relative TEER for each  
450 treatment group. (B) Area under the curve (AUC) calculation for the different treatments. Mean  
451 values of AUC for each group were compared to untreated medium-only control group using one-  
452 way ANOVA + Tukey's test. (C, D) Human endothelial cell monolayers grown in gelatin-coated  
453 coverslips were treated with (C) medium only or (D) 10 ug/mL of YFV NS1 for 3h. After fixation,  
454 cell surface SDC-1 was stained in red and nuclei in blue. (E) Quantification of SDC-1 protein on  
455 to the cells surface was expressed as mean fluorescence intensity (MFI) as shown in panels C and  
456 D. NS1 treatment was compared to medium-only treatment by t-test. Asterisks indicate significant  
457 difference with  $p < 0.05$ .

458

459 **Fig. 5. Correlation analysis of clinical and laboratory data of study participants during acute**  
460 **YF.** (A) Correlation matrix analyzed by Spearman test using a linear model. Asterisks indicate  
461 significant correlations ( $p < 0.05$ , Spearman  $r > 0.35$ ). (B) Correlation between serum levels of YFV  
462 NS1 and sSDC-1. (C) Correlation between serum levels of YFV NS1 and TEER AUC values. (D)  
463 Correlation between serum levels of sSDC-1 and TEER AUC values. Abbreviations: TEER,  
464 transendothelial electrical resistance; AUC, area under the curve; Hb, hemoglobin; Ht, hematocrit;  
465 AST, aspartate transaminase; ALT, alanine aminotransferase; TPI/INR thrombin potential  
466 index/international normalized ratio; aPTT, activated partial thromboplastin time; TB, total  
467 bilirubin; DB, direct bilirubin; IB, indirect bilirubin.

468

469

485 **References**

486

- 487 1. M. U. Kraemer, *et al.*, Spread of yellow fever virus outbreak in Angola and the Democratic  
488 Republic of the Congo 2015–16: a modelling study. *Lancet Infect. Dis.* **17**, 330–338 (2017).
- 489 2. E. G. Kallas, *et al.*, Predictors of mortality in patients with yellow fever: an observational  
490 cohort study. *Lancet Infect. Dis.* **19**, 750–758 (2019).
- 491 3. C. L. Gardner, K. D. Ryman, Yellow fever: a reemerging threat. *Clin. Lab. Med.* **30**, 237–260  
492 (2010).
- 493 4. D. R. Glasner, H. Puerta-Guardo, P. R. Beatty, E. Harris, The good, the bad, and the  
494 shocking: the multiple roles of dengue virus nonstructural protein 1 in protection and  
495 pathogenesis. *Annu. Rev. Virol.* **5**, 227–253 (2018).
- 496 5. D. H. Libraty, *et al.*, High circulating levels of the dengue virus nonstructural protein NS1  
497 early in dengue illness correlate with the development of dengue hemorrhagic fever. *J.*  
498 *Infect. Dis.* **186**, 1165–1168 (2002).
- 499 6. S. A. Paranavitane, *et al.*, Dengue NS1 antigen as a marker of severe clinical disease. *BMC*  
500 *Infect. Dis.* **14**, 570 (2014).
- 501 7. H. T. L. Duyen, *et al.*, Kinetics of plasma viremia and soluble nonstructural protein 1  
502 concentrations in dengue: differential effects according to serotype and immune status. *J.*  
503 *Infect. Dis.* **203**, 1292–1300 (2011).
- 504 8. H. Puerta-Guardo, *et al.*, Flavivirus NS1 Triggers Tissue-Specific Vascular Endothelial  
505 Dysfunction Reflecting Disease Tropism. *Cell Rep.* **26**, 1598-1613.e8 (2019).
- 506 9. H. Puerta-Guardo, *et al.*, Flavivirus NS1 Triggers Tissue-Specific Disassembly of  
507 Intercellular Junctions Leading to Barrier Dysfunction and Vascular Leak in a GSK-3 $\beta$ -  
508 Dependent Manner. *Pathogens* **11**, 615 (2022).
- 509 10. P. Pan, *et al.*, DENV NS1 and MMP-9 cooperate to induce vascular leakage by altering  
510 endothelial cell adhesion and tight junction. *PLoS Pathog.* **17**, e1008603 (2021).

- 511 11. A. W. Wessel, *et al.*, Levels of circulating NS1 impact West Nile virus spread to the brain. *J.*  
512 *Virol.* **95**, e00844-21 (2021).
- 513 12. L. Hui, *et al.*, Matrix metalloproteinase 9 facilitates Zika virus invasion of the testis by  
514 modulating the integrity of the blood-testis barrier. *PLoS Pathog.* **16**, e1008509 (2020).
- 515 13. C.-Y. Lin, *et al.*, High levels of serum hyaluronan is an early predictor of dengue warning  
516 signs and perturbs vascular integrity. *EBioMedicine* **48**, 425–441 (2019).
- 517 14. D. A. Espinosa, *et al.*, Increased serum sialic acid is associated with morbidity and mortality  
518 in a murine model of dengue disease. *J. Gen. Virol.* **100**, 1515–1522 (2019).
- 519 15. H. Puerta-Guardo, *et al.*, Zika Virus Nonstructural Protein 1 Disrupts Glycosaminoglycans  
520 and Causes Permeability in Developing Human Placentas. *J. Infect. Dis.* **221**, 313–324  
521 (2020).
- 522 16. V. Mariappan, S. Adikari, L. Shanmugam, J. M. Easow, A. B. Pillai, Expression dynamics of  
523 vascular endothelial markers: Endoglin and syndecan-1 in predicting dengue disease  
524 outcome. *Transl. Res.* **232**, 121–141 (2021).
- 525 17. H.-R. Chen, *et al.*, Macrophage migration inhibitory factor is critical for dengue NS1-  
526 induced endothelial glycocalyx degradation and hyperpermeability. *PLoS Pathog.* **14**,  
527 e1007033 (2018).
- 528 18. T. H.-C. Tang, *et al.*, Increased serum hyaluronic acid and heparan sulfate in dengue fever:  
529 association with plasma leakage and disease severity. *Sci. Rep.* **7**, 1–9 (2017).
- 530 19. A. D. Theocharis, S. S. Skandalis, G. N. Tzanakakis, N. K. Karamanos, Proteoglycans in  
531 health and disease: novel roles for proteoglycans in malignancy and their pharmacological  
532 targeting. *FEBS J.* **277**, 3904–3923 (2010).
- 533 20. L. Liu, M. Akkoyunlu, Circulating CD138 enhances disease progression by augmenting  
534 autoreactive antibody production in a mouse model of systemic lupus erythematosus. *J.*  
535 *Biol. Chem.* **297**, 101053 (2021).

- 536 21. T. Manon-Jensen, Y. Itoh, J. R. Couchman, Proteoglycans in health and disease: the multiple  
537 roles of syndecan shedding. *FEBS J.* **277**, 3876–3889 (2010).
- 538 22. K. Suzuki, *et al.*, Serum syndecan-1 reflects organ dysfunction in critically ill patients. *Sci.*  
539 *Rep.* **11**, 1–9 (2021).
- 540 23. R. Vollenberg, *et al.*, Indications of persistent glycocalyx damage in convalescent COVID-19  
541 patients: a prospective multicenter study and hypothesis. *Viruses* **13**, 2324 (2021).
- 542 24. D. Zhang, *et al.*, Syndecan-1, an indicator of endothelial glycocalyx degradation, predicts  
543 outcome of patients admitted to an ICU with COVID-19. *Mol. Med.* **27**, 1–12 (2021).
- 544 25. S. Suwanto, R. T. Sasmono, R. Sinto, E. Ibrahim, M. Suryamin, Association of Endothelial  
545 Glycocalyx and Tight and Adherens Junctions With Severity of Plasma Leakage in Dengue  
546 Infection. *J. Infect. Dis.* **215**, 992–999 (2017).
- 547 26. F. Tramontini Gomes de Sousa Cardozo, *et al.*, Serum from dengue virus-infected patients  
548 with and without plasma leakage differentially affects endothelial cells barrier function in  
549 vitro. *PloS One* **12**, e0178820 (2017).
- 550 27. S. B. Biering, *et al.*, Structural basis for antibody inhibition of flavivirus NS1-triggered  
551 endothelial dysfunction. *Science* **371**, 194–200 (2021).
- 552 28. S. Gaudette, D. Hughes, M. Boller, The endothelial glycocalyx: structure and function in  
553 health and critical illness. *J. Vet. Emerg. Crit. Care* **30**, 117–134 (2020).
- 554 29. P. K. Lam, *et al.*, Visual and biochemical evidence of glycocalyx disruption in human dengue  
555 infection, and association with plasma leakage severity. *Front. Med.* **7**, 545813 (2020).
- 556 30. B. Buijsers, *et al.*, Increased plasma heparanase activity and endothelial glycocalyx  
557 degradation in dengue patients is associated with plasma leakage. *Front. Immunol.* **12**,  
558 Article number 759570 (2021).
- 559 31. A. Haynes III, *et al.*, Syndecan 1 shedding contributes to *Pseudomonas aeruginosa* sepsis.  
560 *Infect. Immun.* **73**, 7914–7921 (2005).

- 561 32. H. Joensuu, *et al.*, Soluble syndecan-1 and serum basic fibroblast growth factor are new  
562 prognostic factors in lung cancer. *Cancer Res.* **62**, 5210–5217 (2002).
- 563 33. Z. Malek-Hosseini, S. Jelodar, A. Talei, A. Ghaderi, M. Doroudchi, Elevated Syndecan-1  
564 levels in the sera of patients with breast cancer correlate with tumor size. *Breast Cancer* **24**,  
565 742–747 (2017).
- 566 34. F. A. Olímpio, *et al.*, Endothelium Activation during Severe Yellow Fever Triggers an Intense  
567 Cytokine-Mediated Inflammatory Response in the Liver Parenchyma. *Pathog. Basel Switz.*  
568 **11**, 1–7 (2022).
- 569 35. A.-N. Pelletier, *et al.*, Yellow fever disease severity is driven by an acute cytokine storm  
570 modulated by an interplay between the human gut microbiome and the metabolome.  
571 *medRxiv*, 2021.09.25.21264125 (2021).
- 572 36. A. L. Bailey, *et al.*, Consumptive coagulopathy of severe yellow fever occurs independently  
573 of hepatocellular tropism and massive hepatic injury. *Proc. Natl. Acad. Sci.* **117**, 32648–  
574 32656 (2020).
- 575 37. A. P. Rathore, A. L. St. John, Cross-reactive immunity among flaviviruses. *Front. Immunol.*  
576 **11**, 334 (2020).
- 577 38. M. G. Guzman, *et al.*, Multi-country evaluation of the sensitivity and specificity of two  
578 commercially-available NS1 ELISA assays for dengue diagnosis. *PLoS Negl. Trop. Dis.* **4**,  
579 e811 (2010).
- 580 39. C. A. Schneider, W. S. Rasband, K. W. Eliceiri, NIH Image to ImageJ: 25 years of image  
581 analysis. *Nat. Methods* **9**, 671–675 (2012).
- 582 40. C. Ritz, F. Baty, J. C. Streibig, D. Gerhard, Dose-response analysis using R. *PloS One* **10**,  
583 e0146021 (2015).
- 584 41. W. J. Conover, *Practical nonparametric statistics* (John Wiley & Sons, 1999).
- 585 42. J. M. Chambers, A. Freeny, R. M. Heiberger, “Linear models” in *Statistical Models*, (J. M.

586 Chambers and T. J. Hastie, Wadsworth & Brooks/Cole., 1992).

587 43. W. S. Cleveland, E. Grosse, W. M. Shyu, “Local regression models” in *Statistical Models*, (J.

588 M. Chambers and T. J. Hastie, Wadsworth & Brooks/Cole., 1992).

589

**Table 1: Demographic, clinical, and laboratory data of study participants**

	Control (n=11)	Non-severe (n=18)	Severe <sup>#</sup> (n=39)	p-value (Non-severe vs Severe)
<b>Age (years)</b>	38 (22 - 67)	39 (19 - 74)	42 (18 - 72)	ns $p=0.9039$
<b>Gender (male)<sup>a</sup></b>	4 (36.36%)	16 (88.89%)	35 (89.74%)	ns $p=0.9959$
<b>Days after symptom onset<sup>b</sup></b>	-	9 (6 - 24)	7 (3 - 20)	* $p=0.0245$
<b>Hospitalization<sup>a</sup></b>	-	11 (61.11%)	31 (79.49%)	ns $p=0.1975$
<b>Viral load (genomic RNA copies/mL)</b>	-	$1.04 \times 10^3$ ( $3 - 2.50 \times 10^4$ )	$2.03 \times 10^5$ ( $7 - 2.22 \times 10^8$ )	**** $p=0.0001$
<b>Leukocyte count<sup>c</sup></b>	nd	3.72 (1.35 - 6.78)	4.22 (1.44 - 17.09)	ns $p=0.1782$
<b>Lymphocyte count<sup>c,d</sup></b>	nd	1.06 (0.26 - 2.14)	0.80 (0.21 - 2.19)	ns $p=0.1119$
<b>Neutrophil count<sup>c</sup></b>	nd	1.75 (0.38 - 3.79)	2.98 (0.99 - 14.88)	** $p=0.0061$
<b>Platelet count<sup>c,d</sup></b>	nd	89.00 (43.00 - 328.00)	67.00 (17.00 - 361)	ns $p=0.1005$
<b>Hemoglobin (Hb, g/dL)<sup>d</sup></b>	nd	13.90 (7.20 - 16.50)	13.70 (6.40 - 18.20)	ns $p=0.5454$
<b>Hematocrit (Ht, %)<sup>d</sup></b>	nd	40.85 (21.30 - 48.30)	38.95 (18.90 - 52.40)	ns $p=0.3814$
<b>Aspartate transaminase (AST, U/L)</b>	nd	521.5 (40 - 2510)	3736 (138 - 21721)	*** $p=0.0002$
<b>Alanine aminotransferase<sup>e</sup> (ALT, U/L)</b>	nd	753 (42 - 2677)	2232 (59 - 8822)	** $p=0.0060$
<b>Creatinine<sup>d</sup> (mg/dL)</b>	nd	0.97 (0.44 - 1.52)	2.98 (0.65 - 10.50)	*** $p=0.0004$
<b>Fibrinogen<sup>g</sup> (mg/dL)</b>	nd	184 (96 - 309)	138 (52 - 560)	ns $p=0.2217$
<b>PT/INR<sup>d</sup></b>	nd	1.06 (0.94 - 1.78)	1.30 (0.95 - 3.51)	**** $p=0.0001$
<b>aTTP<sup>f</sup> (s)</b>	nd	30.90 (23.90 - 39.50)	38.85 (21.70 - 200)	** $p=0.0012$
<b>Total bilirubin (TB, mg/dL)<sup>d</sup></b>	nd	1.04 (0.28 - 6.00)	4.72 (0.11 - 30.96)	** $p=0.0025$
<b>Direct bilirubin (DB, mg/dL)<sup>d</sup></b>	nd	0.92 (0.16 - 5.88)	4.10 (0.15 - 27.16)	** $p=0.0040$
<b>Indirect bilirubin (IB, mg/dL)</b>	nd	0.15 (0.01 - 0.50)	0.62 (0.06 - 7.45)	* $p=0.0124$
<b>Death<sup>a</sup></b>	-	0 (0%)	17 (42.50 %)	*** $p=0.0006$

Data are shown as median (range). Groups were compared by Mann-Whitney (two groups) or Kruskal-Wallis (three groups) test.

<sup>a</sup> Gender, hospitalization, and death are reported as number of patients per group (percentage of total within each group).

<sup>b</sup> All the samples were collected upon hospital admission, and the days after symptom onset was determined based on patient report at admission.

<sup>c</sup> Leukocyte, lymphocyte, neutrophil, and platelet count are shown as number  $\times 10^3/\text{mm}^3$  of blood.

<sup>d</sup> Data missing for one patient.

<sup>e</sup> Data missing for two patients.

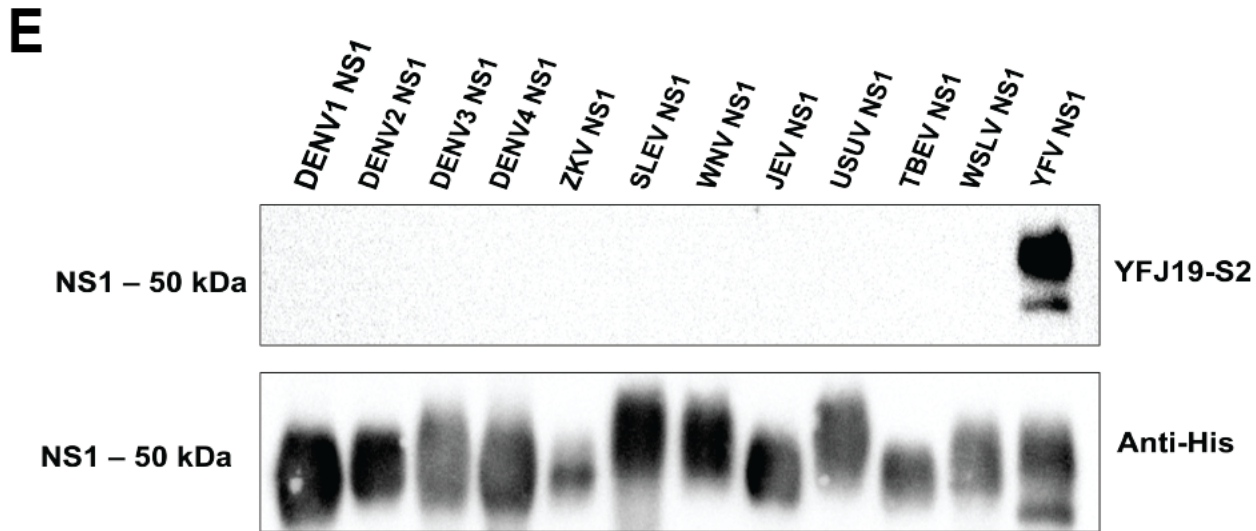
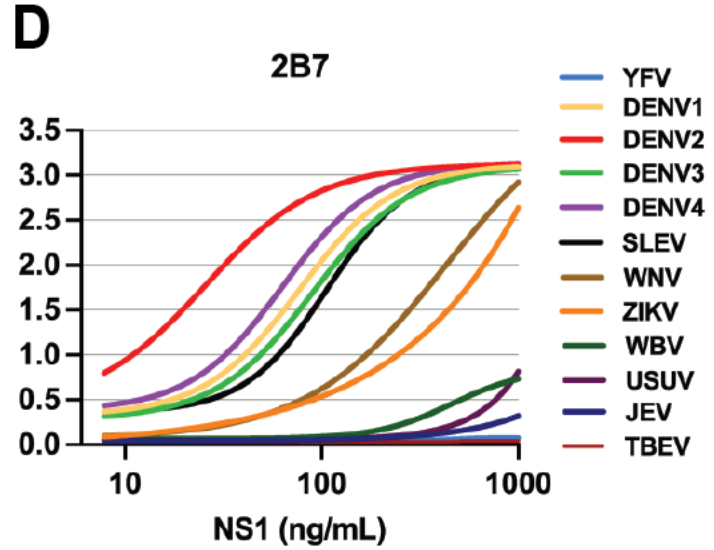
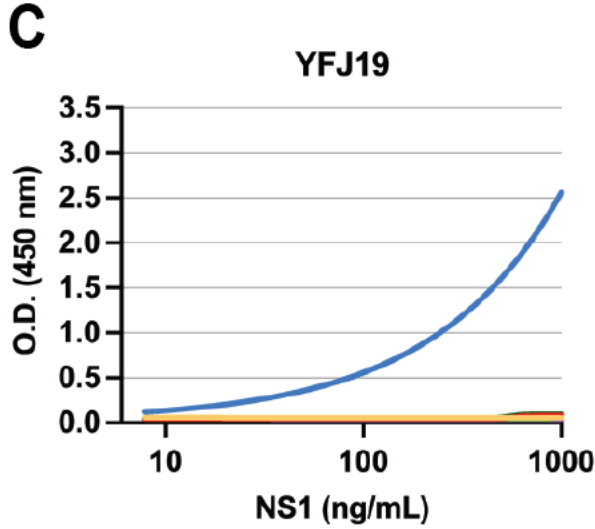
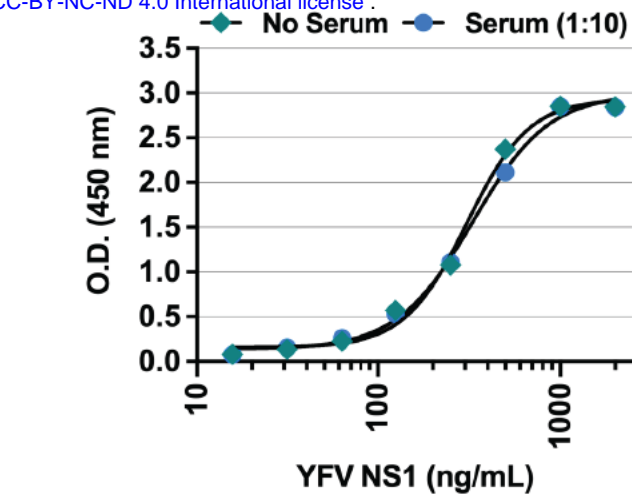
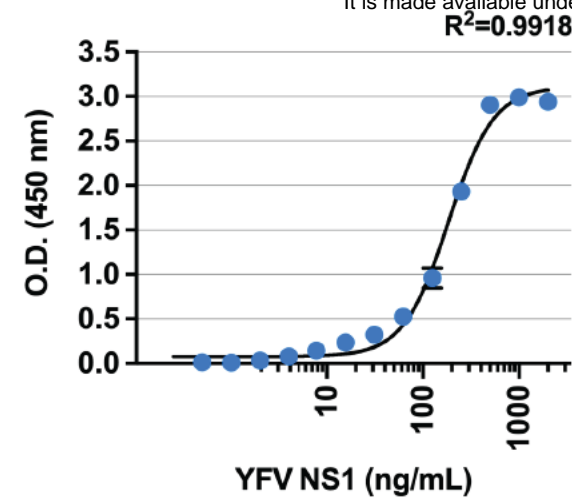
<sup>f</sup> Data missing for six patients.

<sup>g</sup> Data missing for nine patients.

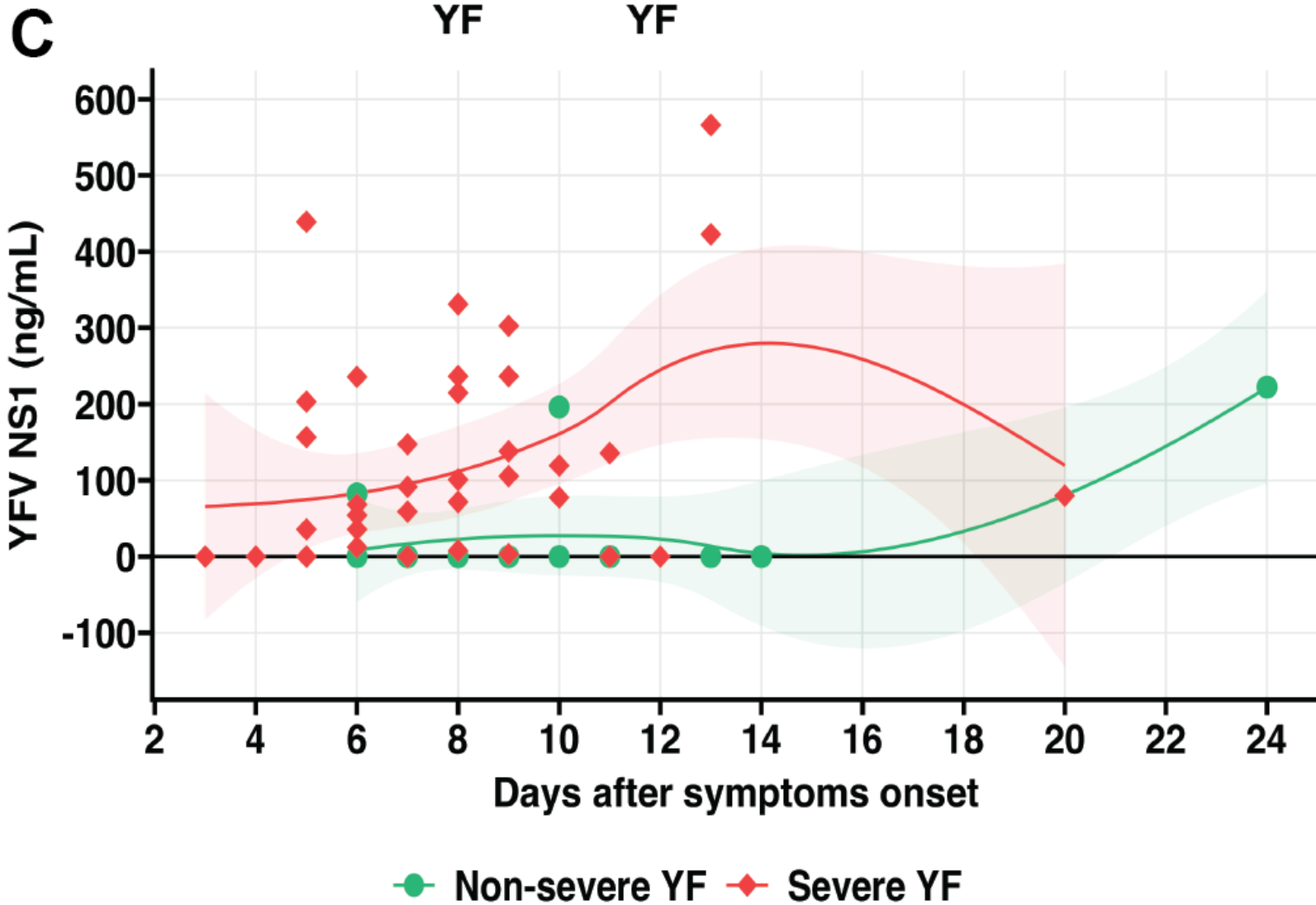
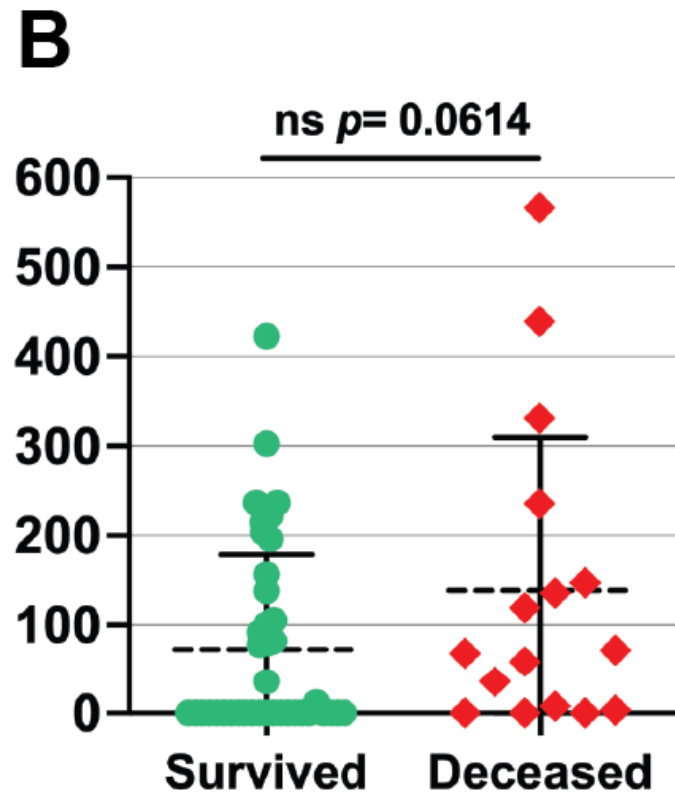
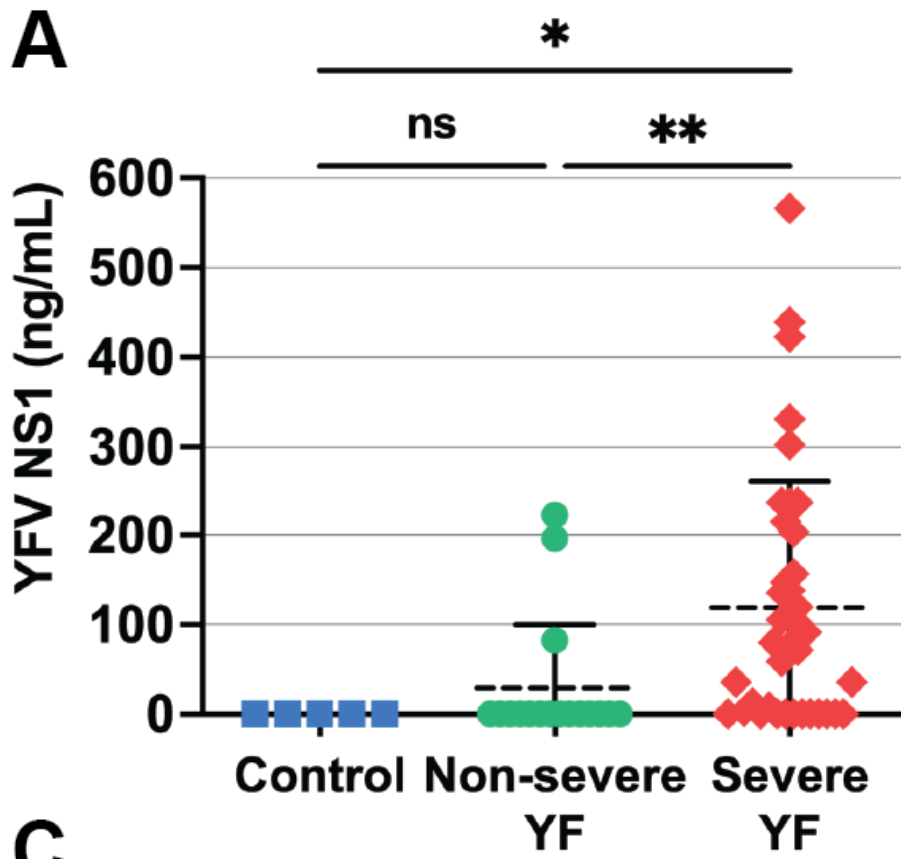
\* significant  $p$ -value.

Abbreviations: nd, not determined; ns, not significant; PT/INR: Prothrombin Time/International Normalized Ratio; aTTP, Activated Partial Thromboplastin Clotting Time.

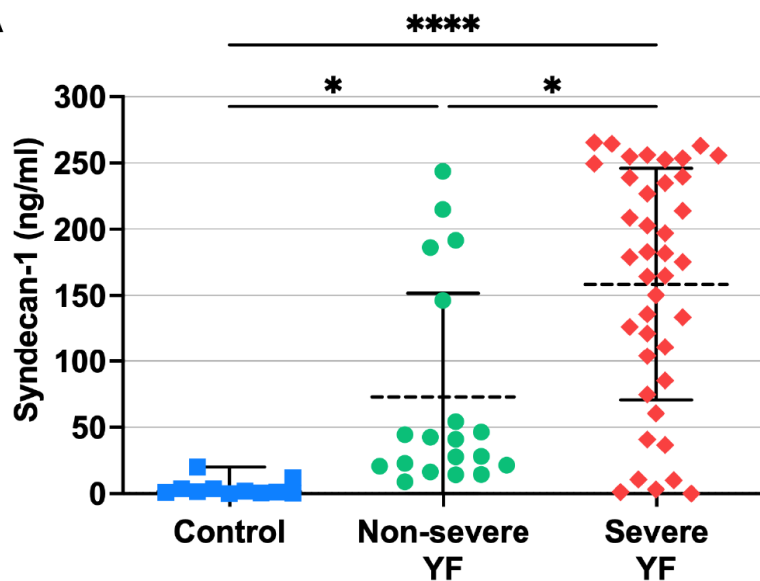
<sup>#</sup> Liver transplant was required for one patient from the severe group.



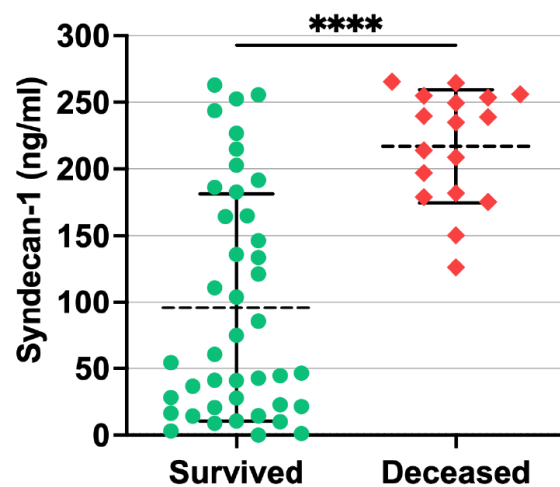




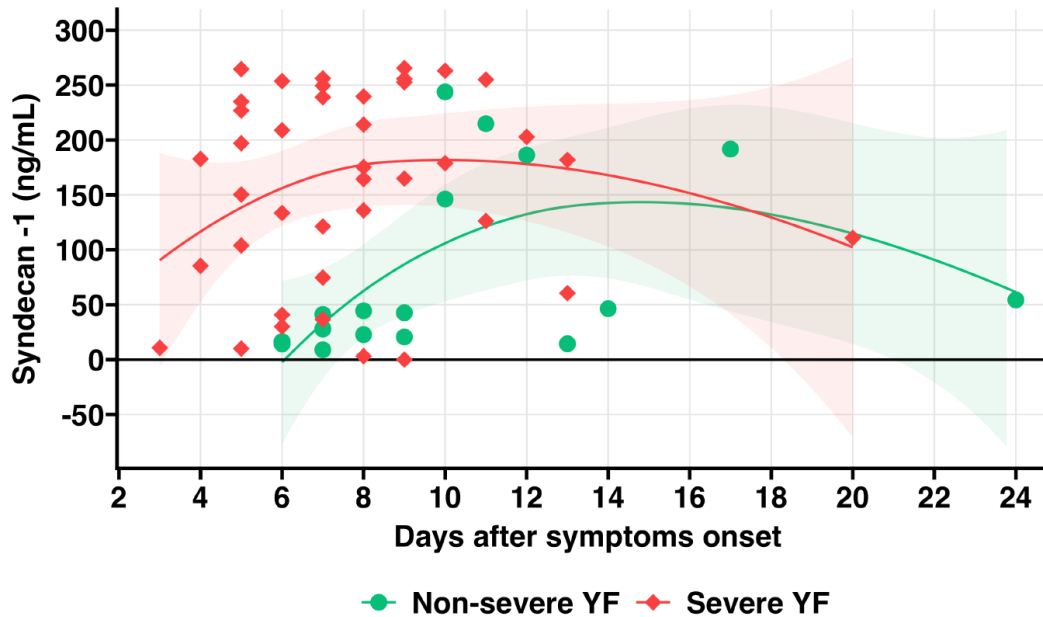
**A**



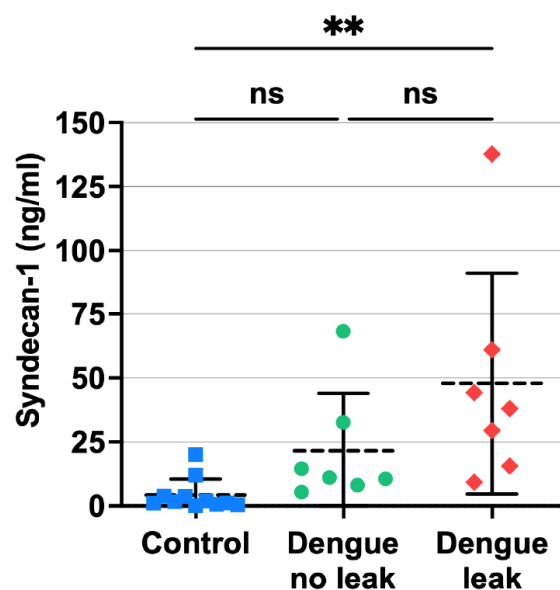
**B**

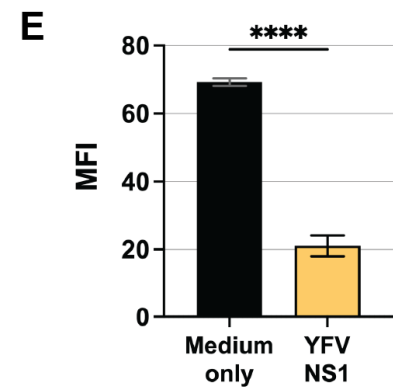
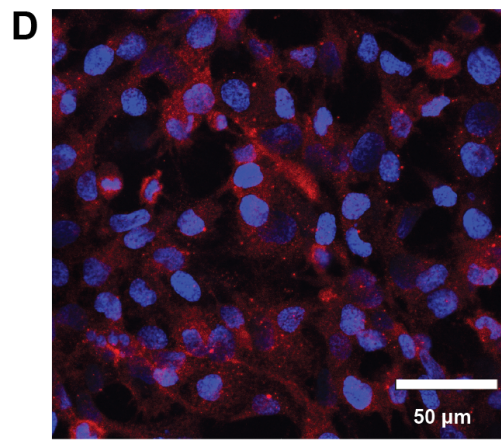
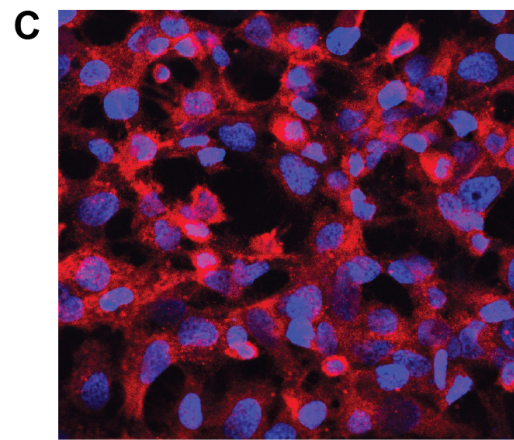
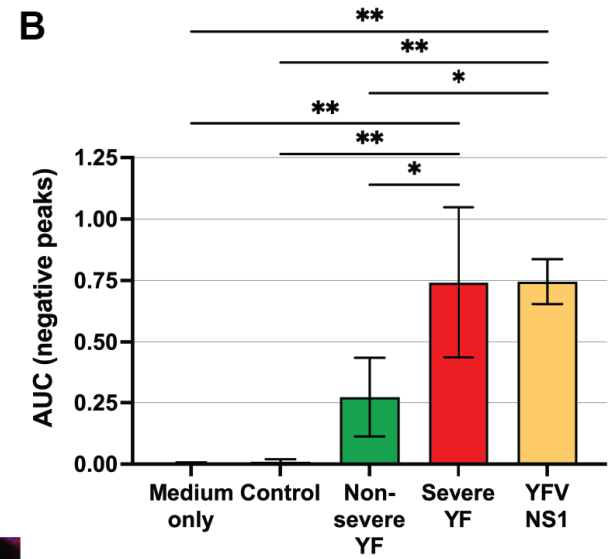
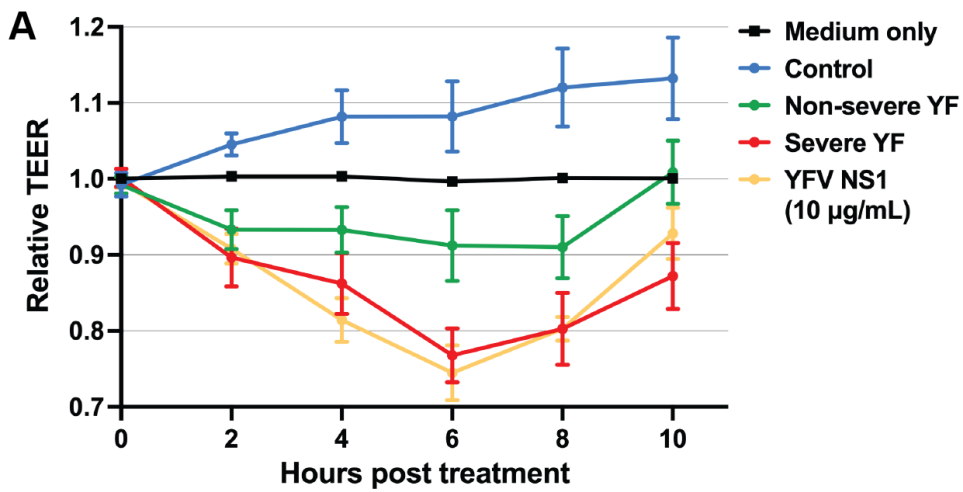


**C**

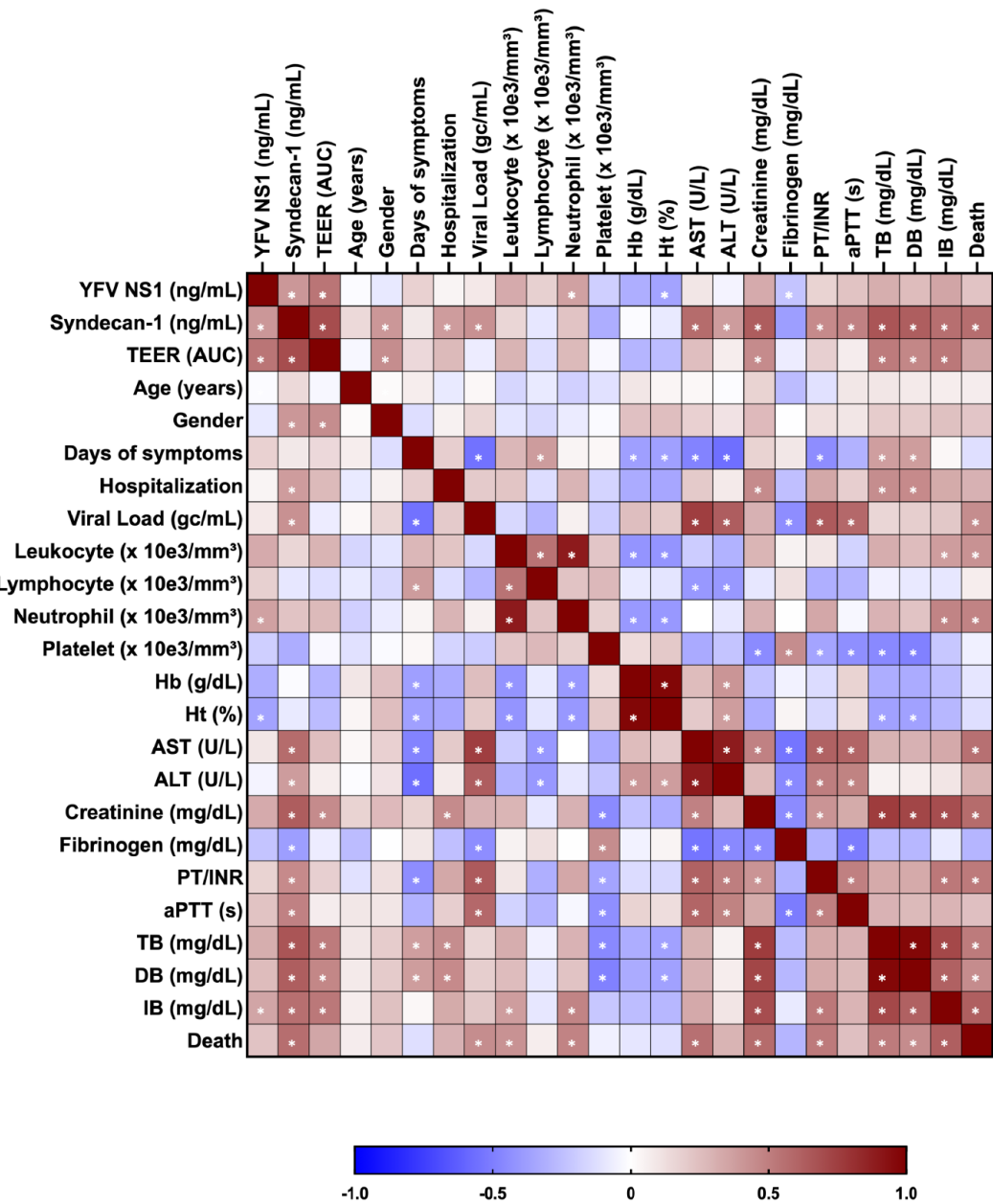


**D**

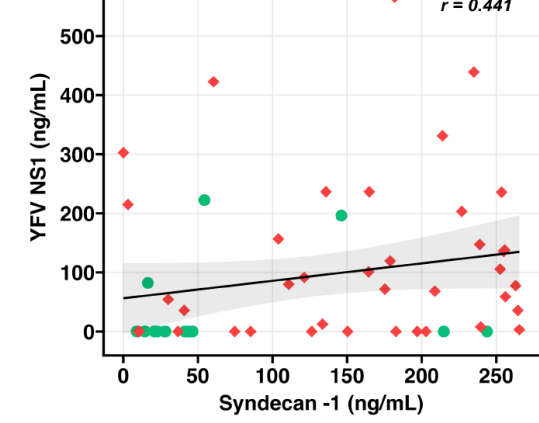




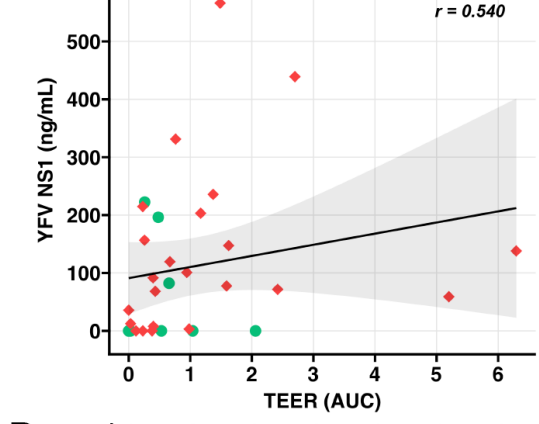
**A**



**B**



**C**



**D**

